Molecular Biology Reports (2024) 51:482
https://doi.org/10.1007/s11033-024-09394-9

ORIGINAL ARTICLE

Harnessing potential of avian eggshell membrane derived collagen hydrolysate for bone tissue regeneration

Aakriti Aggarwal[1] · Debasish Nath[2] · Asish Pal[2] · Mahesh Kumar Sah[1]

Received: 10 November 2023 / Accepted: 28 February 2024

Abstract

Background Natural bone grafts are the highly preferred materials for restoring the lost bone, while being constrained of donor availability and risk of disease transmission. As a result, tissue engineering is emerging as an efficacious and competitive technique for bone repair. Bone tissue engineering (TE) scaffolds to support bone regeneration and devoid of aforesaid limitations are being vastly explored and among these the avian eggshell membrane has drawn attention for TE owing to its low immunogenicity, similarity with the extracellular matrix, and easy availability.

Methodology and results In this study, the development of bone ingrowth support system from avian eggshell membrane derived collagen hydrolysates (Col-h) is reported. The hydrolysate, cross-linked with glutaraldehyde, was developed into hydrogels with poly-(vinyl alcohol) (PVA) by freeze-thawing and further characterized with ATR-FTIR, XRD, FESEM. The biodegradability, swelling, mechanical, anti-microbial, and biocompatibility evaluation were performed further for the suitability in bone regeneration. The presence of amide I, amide III, and -OH functional groups at 1639 cm^{-1},1264 cm^{-1}, and 3308 cm^{-1} respectively and broad peak between 16°-21° (2θ) in XRD data reinstated the composition and form.

Conclusions The maximum ratio of Col-h/PVA that produced well defined hydrogels was 50:50. Though all the hydrogel matrices alluded towards their competitive attributes and applicability towards restorative bone repair, the hydrogel with 40:60 ratios showed better mechanical strength and cell proliferation than its counterparts. The prominent *E. coli* growth inhibition by the hydrogel matrices was also observed, along with excellent biocompatibility with MG-63 osteoblasts. The findings indicate strongly the promising application of avian eggshell-derived Col-h in supporting bone regeneration.

Keywords Eggshell membrane · Collagen hydrolysate · Enzymatic hydrolysis · Hydrogel matrices · Bone tissue engineering

Abbreviations

PVA	Poly-(vinyl alcohol)
TE	Tissue engineering
ESM	Eggshell membrane
ECM	Extracellular Matrix
3-MPA	3-mercaptopropionic acid
PBS	Phosphate buffer saline
F-T	Freeze-thaw

✉ Mahesh Kumar Sah
sahmk@nitj.ac.in

[1] Department of Biotechnology, Dr. B. R. Ambedkar National Institute of Technology, Jalandhar, Punjab 1440081, India

[2] Chemical Biology Unit, Institute of Nanoscience and Technology, Sector 81, Mohali, Punjab 140306, India

Introduction

Natural bone grafts such as autografts and allografts are preferred for bone restoration applications; nevertheless, they are constrained in terms of donor availability and involve a risk of disease transmission [1]. As a result, biomedical research is keenly focusing on bone tissue regenerative scaffolds which can simulate the biochemical properties of the extracellular matrix (ECM) of the bone and can induce molecular cues for osteoinduction and osteoconduction [2]. The major portion of the organic content of the ECM of bone is collagenous, which aids in cell anchoring and regulates osteoblasts' growth [3]. To facilitate the regeneration of bone tissue, a scaffold's structure and composition should promote cellular adhesion, proliferation, and differentiation. The ideal scaffold would comprise a design that is optimal for stability without sacrificing bioactivity and

physico-chemical resemblance to the organic mineralized matrix structure of bone [4].

The fabrication of bone TE scaffolds has been vastly explored from both natural and synthetic materials [5]. Despite their exuberant mechanical strength, synthetic polymer-based scaffolds are limited in their application due to the acidic character of their byproducts and their poor attachment to biological moieties [6]. Natural polymers with excellent bioactivity, hydrophilicity, and ECM-like properties, such as silk fibroin [2], chitosan [7], gelatin [8], collagen [9] and others, circumvent the limitations listed above. Among these, collagen being an essential component of bone, also possesses low immunogenicity, optimal porosity, processability, and availability; making it one of the commonly employed biopolymers for wide range of TE applications [10]. Besides, the collagen peptides have also been reported to promote proliferation and differentiation of preosteoblasts by activating the PI3K/Akt (phosphatidylinositol 3kinase)signaling pathway [11]. Bovine and porcine are the main sources of extracting collagen [12], with the extraction methodologies being strenuous and the harvested collagen offering a risk of prion's transmission [13]. Collagen extraction from the avian eggshell membrane (ESM) is gaining momentum due to its wide accessibility, absence of the aforesaid limitations; along with the optimum mechanical and biological properties, -making it an appropriate starting material for the development of bone regeneration matrices. The extraction is sustainable, in addition to ESM being well known to provide physico-chemical cues to effect crucial signaling molecules (transforming growth factors) for promoting specific cell behaviors [14]. Recent studies have reported the utilization of ESM-hydroxyapatite scaffolds to enhance the alkaline phosphatase activity expression of osteogenesis-related genes, and proteins in MC3T3-E1 cells [15]. The scaffolds developed from nanofibers of ESM solution have also reportedly shown an increased potential in regenerating the bone tissue [16]. In addition, the soluble ESM has also shown osteogenic differentiation of mesenchymal stem cells and bone regeneration in mice models [2].

Besides, utilization of ESM for obtaining protein fractions, (including hydrolyzed collagen) also contributes to a circular economy as the eggshell waste gets effectively valorized after the eggs are used by the food industry [9, 17]. However, the collagen needs to be composited with an appropriate polymer to give optimum strength to the bone TE construct.

The article henceforth focuses on the development and utilization of avian ESM derived collagen hydrolysate based hydrogels, by blending with poly-(vinyl alcohol) (PVA) in studying their effects on bone tissue regeneration potential.

Materials and methods

Materials

The chicken eggshells were sourced from the NIT Jalandhar Institute Canteen in Punjab, India. PVA (Mw 60,000, degree of hydrolysis ≥ 98%) was obtained from Merck™. Pepsin (1000U/mg) from porcine was obtained from Hi-Media™. The analytical grade 3-mercaptopropionic acid (3-MPA), acetic acid, and NaOH were also supplied by Hi-Media™. The osteoblast cell line for study was obtained from NCCS, Pune (India). The cell culture reagents MTT (3-(4, 5-dimethylthiazolyl-2)-2, 5-diphenyltetrazolium bromide), Dulbecco's Minimum Essential Medium Eagle (DMEM), Fetal Bovine Serum (FBS), Penicillin-Streptomycin, Fluorescein diacetate (FDA), and Propidium iodide (PI) were purchased from TCI™, Cytive™, Gibco™, Hi-Media™, Merck™, and Hi-Media™, respectively.

Methods

The collagen extraction process

The eggshells washed with water, were utilized for the manual peeling of the ESM, which were further chemically processed to remove the soluble ESM protein fractions, as described in our previous work [18]. In brief, the ESM were hydrolyzed in an acidic environment with 0.5 M 3-mercaptopropionic acid (3-MPA) and 10% acetic acid, and the solubilized protein was precipitated using NaOH. The remaining ESM fractions (predominantly collagenous), were further ultrasonicated in distilled water (0.5% w/V) at a frequency of 38 kHz for 1 h [9]. The uniform suspension was then enzymatically hydrolyzed by utilizing pepsin (500 U), and incubating the system at 37 °C for 4 days. 0.5 M acetic acid was used to maintain the pH of the system at 3, throughout the hydrolysis process. The collagen solution obtained is hereafter referred to as collagen hydrolysate (Col-h).

Development of Col-h based hydrogels

The Col-h was mixed with PVA (14% w/V) with varying ratios, as shown in Table 1. The Col-h/PVA blends were magnetically stirred for 8 h at 20°C, in the presence of 0.5% glutaraldehyde as the crosslinker. The blends were thereafter neutralized using 1 M NaOH, prior to their hydrogels' formation through 7 freeze-thaw cycles at -20°C for 8 h and 25°C (RT) for 3 h [9, 19]. The hydrogels, for each blend type were prepared in triplicates; and lyophilized at -80°C (FreeZone, LABCONCO), for obtaining the freeze-dried forms before their further physico-chemical characterization.

Table 1 Ratio of collagen and PVA in the blends, along with their respective hydrogel codes

Sample codes	Col-h:PVA (V/V)
H1	**10:90**
H2	**20:80**
H3	**30:70**
H4	**40:60**
H5	**50:50**
H6	**60:40**

Attenuated total reflectance-fourier transform infrared (ATR-FTIR) spectroscopy

An ATR-FTIR spectrophotometer (Bruker, Alpha II-Platinum) was used to determine the hydrogels' chemical composition. The transmission spectra were averaged for 40 scans in the wavelength range of 600–4000 cm^{-1}.

X-ray diffraction (XRD)

PAnalytical Empyrean XRD was used to investigate the hydrogels' elemental constitute. The lyophilized hydrogels were scanned using collimated Cu-K rays, at a rate of 2 degrees per minute from $2\theta = 5–28°$ [9].

Field emission scanning electron microscopy (FESEM)

FESEM (Zeiss, SIGMA 500VP) was used for the assessment of the morphological properties of the hydrogels. The lyophilized hydrogels were gold coated before proceeding for the imaging process. The surface images of the hydrogel samples were next analyzed for the average pore sizes, surface topological roughness values and average percentage porosity with ImageJ software [20, 21], as described in our earlier reports [9, 18].

Biodegradability

The hydrogels' degradation was investigated by initially weighing the lyophilized hydrogels (Wi), then immersing them in Phosphate buffer saline (PBS, pH 7.2) at 37 °C for 7, 14, 21, and 28 days. The contamination was prevented by replacing the PBS solution every second day [22]. The hydrogels received removal at the specified time intervals and then lyophilized to calculate the final weight (W_f). Equation 1 was used to compute the degradation rate further [22].

$$\text{Degradation Rate } (\%) = \frac{W_i - W_f}{W_i} \times 100 \quad (1)$$

Swelling index

The swelling index of the hydrogels was assessed by their ability to absorb water. After weighing the lyophilized hydrogels (W_i), they were allowed complete immersion in water for 5, 10, 20, 40, 60, 120, and 1440 min. Following immersion, the hydrogels were removed and the surface moisture was dried with a tissue paper. Next, the hydrogels were weighed to obtain the final weight (W_f), and the swelling index was then computed using Eq. 2 [22].

$$\text{SwellingIndex } (\%) = \frac{W_f - W_i}{W_i} * 100 \quad (2)$$

Tensile strength measurement

The mechanical properties of the hydrogel films were evaluated as per the ASTM D638 standards using an automated universal testing machine (Ashian Engineers Company India, 2 KN) [23]. The test films of 4.5 cm length, and 0.2 cm width were fixed; and the tension was applied until the breaking point. The measurements from three replicates ($n = 3$) were averaged to assess the tensile strength and percentage elongation of all the hydrogel film samples.

Anti-microbial studies

The bacterial strain of *E. coli* was inoculated in 10 ml of luria broth (LB) media and cultured overnight in a BOD incubator at 37 °C. This culture was further employed to test the antibacterial properties of Collagen/PVA blends; using the disc diffusion method. The *E. coli* culture was evenly spread throughout the entire sterile agar surface of a dried Luria agar plate to inoculate it. The impregnated discs were filled with varying concentrations of hydrogel precursor solutions, incubated for 24 h at 37°C, and then observed for growth. The diameter of the total inhibitory zones on the disc was measured to assess the antibacterial activity.

In–vitro cell proliferation, cytotoxicity, and viability assessment

The MTT (3-(4, 5-dimethylthiazolyl-2)-2, 5-diphenyltetrazolium bromide) test on MG-63 osteoblast cells was used to assess the hydrogels' in-vitro cytotoxicity. A sub confluent monolayer of the cells was created by seeding them at a density of 1×10^4 cells/well in a 96-well-plate with 100 µL of Dulbecco's Minimum Essential Medium Eagle (DMEM), 10% Fetal Bovine Serum, and 1% Penicillin-Streptomycin; with further incubation at 37 °C and 5% carbon dioxide (CO_2). The culture medium was next replaced with hydrogel

extracts, and a negative control (PVA) (all prepared in the culture medium) after 24 h. After the completion of treatment period of 24 h, 50µL of MTT solution (1 mg/ml) was put in each well and incubated further for two hours. The MTT solution was subsequently removed and the formazan that was produced as a result of the metabolic breakdown of MTT by living cells was dissolved by adding 100 µl of isopropanol. The process was then quantified by measuring the absorbance values of formazaan at 570 nm with the help of an automated microplate reader (BioTek Cytation 5) [24]. The process was also carried out at day 3 and day 7 to assess the cell proliferation.

Fluorescence-based FDA/PI assays were used to investigate the visual proliferation and cellular viability in hydrogels' extracts. Fluorescein diacetate (FDA) and propidium iodide (PI) were used for staining the live and dead cells, respectively [24].The cellular viability and morphology were visualized when the MG-63 osteoblasts, treated with the 100 µl of the hydrogels' (H3, H4, and H5) extract (prepared by dispersing 10 mg/ml hydrogels in culture media) for 7 days were stained. The staining was performed by removing the media, followed by addition of 100 µl of both FDA and PI, with a couple of PBS washings in between. The staining was carried out for 5 min in the cell culture incubator, post which the cells were washed with PBS and later reconstituted in Opti-MeM (Invitrogen), for subsequent imaging under inverted fluorescence microscope [24].

Analysis of variance (ANOVA)

Three separate experiments were used to measure the cell viability data, and the results were presented as mean ± standard deviation. One- way ANOVA was used for the statistical analysis; along with Tukey's HSD and differences with a p-value of 0.05 or less were considered significant.

Results

The residual collagenous portion of the chicken ESM was suspended in water to make a system of uniform collagen dispersion after the soluble protein content was eliminated through acid treatment. The subsequent hydrolysis with enzymatic action of pepsin yielded 0.8 mg/ml Col-h solution, further blend with PVA and cross-linked using glutaraldehyde. The physical crosslinking through seven F-T cycles occurred via the interaction and entanglement of the PVA molecular chains at low temperatures [25], henceforth leading to the development of easy to handle hydrogels, barring H6 which was too mushy. Henceforth, H6 could only be evaluated for the presence of the functional groups and its degradation.

ATR-FTIR analysis

The ATR-FTIR measurements were used for assessing the chemical constitution of the Col-h and PVA (Figure S1). The Col-h showed the presence of C-O or C-C stretching at 1090 cm^{-1} (Figure S1). The peaks at 1636 cm^{-1} and 1219 cm^{-1} corresponded to the amide I and amide III peaks respectively. The vibrational peak at 1323 cm^{-1} is attributed to the CH_2 side chain, which is a characteristic feature of collagen [26]. The C-H stretch in CH_3 gave rise to the peak at 2934 cm^{-1}. The presence of -OH groups caused the peak at 3288 cm^{-1}. Furthermore, the PVA showed the presence of CH_2 rocking at 864 cm^{-1}, C-O-C stretch at 1062 cm^{-1}, C-H bend at 1460 cm^{-1}, C-H stretch at 2923 cm^{-1}, and OH stretching at 3639 cm^{-1}**(Figure S1)** [27, 28].

The assessment of the developed hydrogels showed the stretching of C-O or C-C in collagen and PVA, causing the peak at 1095 cm^{-1} [28]. Another distinctive PVA peak at 1400 cm^{-1} occurred due to the presence of the -CH_2 group. In addition, the C-H stretch in CH_3 gave rise to the peak at 2934 cm^{-1} [29]. All sample groups showed the amide I and amide III peaks at 1639 cm^{-1} and 1264 cm^{-1} respectively [9, 30] which supported the existence of charged functional moieties in the collagen protein. A large, broad peak at 3308 cm^{-1} additionally revealed the significant presence of the -OH and -NH groups [30] in the PVA and collagen molecules, respectively (Fig. 1).

XRD measurements

The hydrogels were further analyzed through the XRD technique, which showed the presence of four peaks at $2\theta = 19.69$, 21.59, 23.10, and 23.94° (***Figure S2***) [31]. The diffraction peaks were attributed to the existence of PVA crystallites localized in the knots of the network structure. The F-T process causes the formation of knots and porous walls in the hydrogel [31], as can also be seen in the FESEM images of the hydrogels (Fig. 2). In addition, a broad peak ranging from 16° to 21° was also observed. This could be attributed to the amorphous nature of the collagen hydrolysate, as also reported previously [9]. This analysis was significant in providing an insight into the ease of Col-h release from the hydrogel matrix. Encapsulation within an amorphous matrix leads to higher release rates in comparison to a crystalline matrix; as the latter requires energy for breaking the crystal lattice during dissolution [32].

FESEM analysis

The hydrogels' morphology was further investigated using FESEM, with all of them displaying well-connected pores (Fig. 2***)***, with the inset showing the size distribution of 20

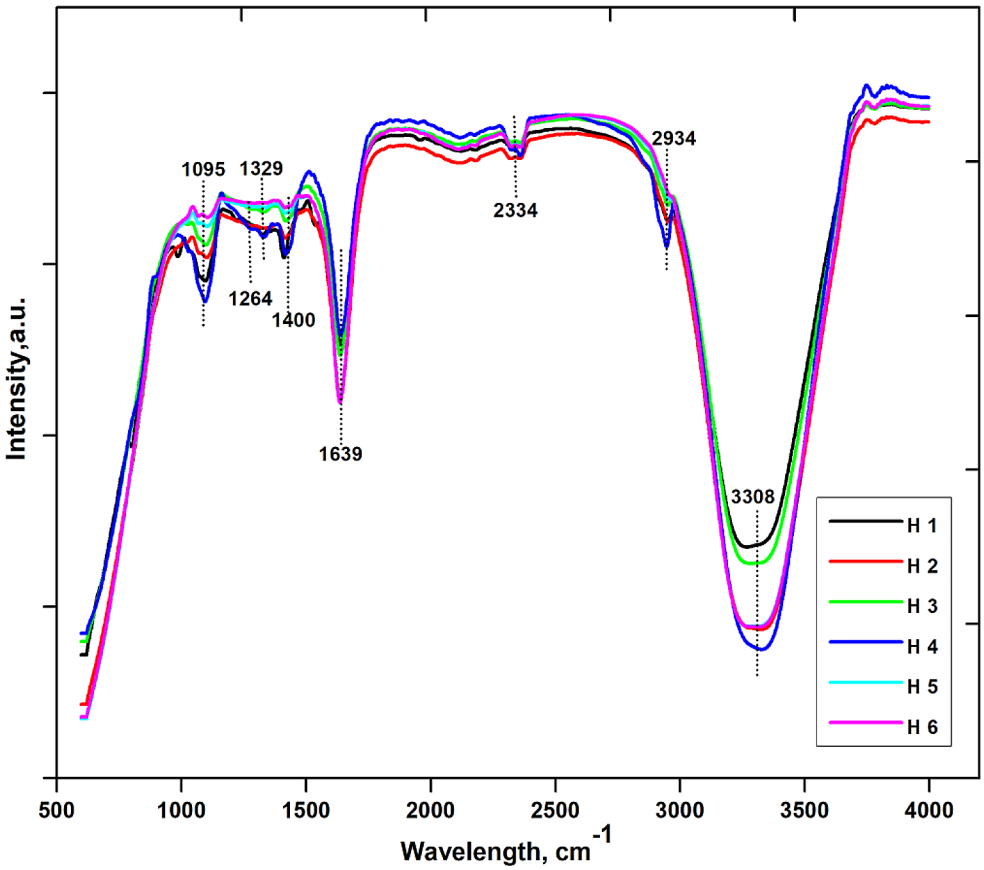

Fig. 1 The ATR-FTIR spectra of the hydrogels H1 to H6, averaged for 40 scans

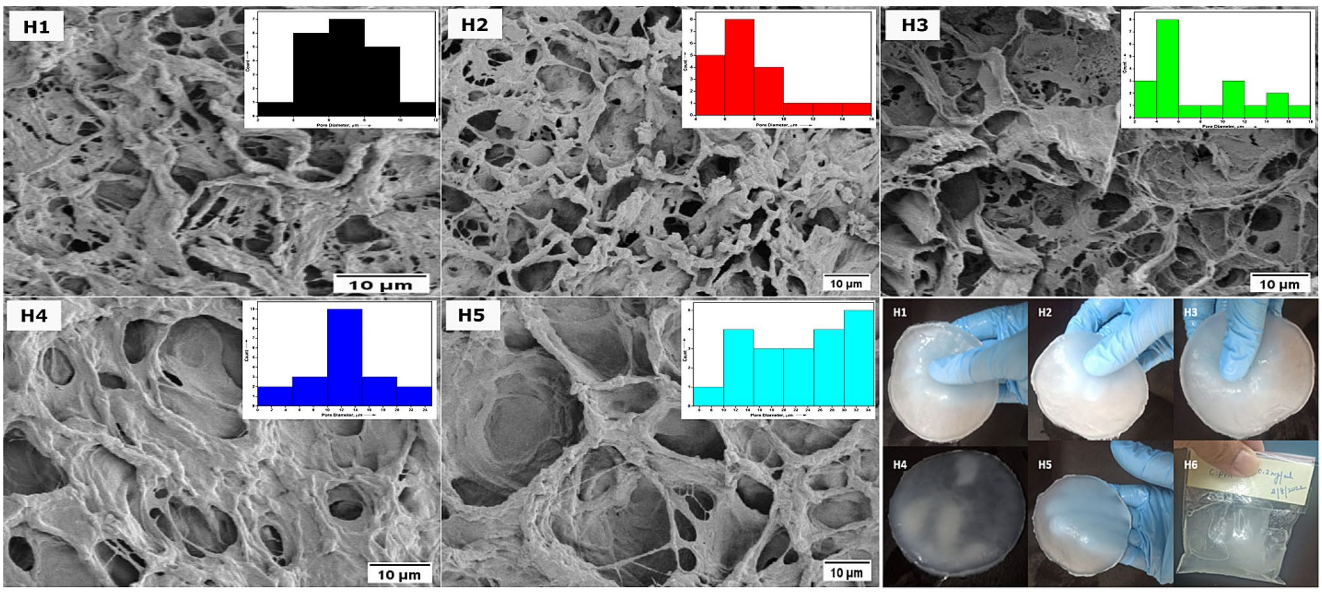

Fig. 2 The FESEM images of the hydrogels H1 to H5 (inset images represent the pore size distribution); along with the real images of the developed hydrogels H1 to H6

randomly selected pores). A comprehensive evaluation of the micrographs was carried out in order to gain an understanding of the microstructural characteristics, such as average pore diameter, percentage porosity, and surface roughness (Table 2), which have a significant contribution towards cell adhesion and proliferation. The surface morphological analysis revealed that the average pore diameters increased from H1 to H5, with the lowest being 6.60 ± 1.90 µm in H1

Table 2 The microstructural analysis of the hydrogels

Hydrogel type	Pore Diameter (Mean ± SD), µm	Percentage Porosity	Average surface roughness, µm
H1	6.60 ± 1.90	55.79	34.26
H2	8.05 ± 2.94	59.17	39.60
H3	8.08 ± 4.90	66.59	38.46
H4	13.3 ± 6.54	64.32	29.38
H5	22.36 ± 8.12	68.96	32.60

to the largest being 22.36 ± 8.12 µm in H5. This may be due to the increased concentration of Col-h, not forming crosslinks with the PVA molecules and remaining as independent structures; thus leading to the increase in pore size of the hydrogel systems [26]. The percentage porosity, which corresponded to the area occupied by the pores present in an area selection of 10 µm × 10 µm in the FESEM images of all the hydrogel sample groups, was calculated through ImageJ as discussed previously. A likewise increasing trend was also visible in case of percentage porosity values (Table 2). Such topological features, including the micrometer ranged surface roughness values of the hydrogels, have been known to stimulate the formation of bone cells. This occurs due to the increased specific surface area offered by the focal adhesion sites, which in turn can facilitate improved cell attachment and dissemination [33].

Biodegradation study

Furthermore, studies on the progressive degradation of the hydrogels revealed weight loss ranging from 10 ± 0.5% for H1 to 44.4 ± 2.2% for H5 after 28 days of hydrogels' immersion in PBS (Fig. 3A). The rate of degradation increased with increase in Col-h content, and is also known to be effected by the extent of crosslinking and porosity [34]. The higher Col-h content may lead to larger pore sizes [26] and weaker interconnections among the molecular chains, thus leading to ease of degradation. It was also seen that H1 and H2, the most tightly bound hydrogels among their counterparts started degrading only after 14 and 7 days respectively, owing to their compact network structures. The H6 degraded completely in 21 days, showing its inability to function as a material for bone regeneration and was hence eliminated in other measurements and studies.

Swelling ability

The ability of the hydrogels for fluid uptake was also analyzed through their swelling properties. The water absorption by the hydrogels was studied at various time intervals till 24 h, with the H5 showing the maximum rate of 257.14 ± 12.85%. In contrast, the H1's uptake was found to be 94.44 ± 4.72%, as shown in Fig. 3B. The higher swelling ability of H5 can be attributed to the presence of higher amount of Col-h which leads to enhanced hydrophilicity in the hydrogels [34]. The higher pore sizes and percentage porosity of H5 (Table 1), w.r.t. its counterparts also conformed to the above analysis. The higher amount of PVA, on moving from H4 to H1, contributed towards much denser hydrogels and correspondingly lesser swelling [35, 36].

Tensile strength analysis

The tensile strength measurements of the hydrogels were next assessed to ascertain their role in load bearing for effective bone regeneration. The ultimate tensile strength and percentage elongation of the hydrogels is shown in Table 3. The measurements revealed the decrease in strength of

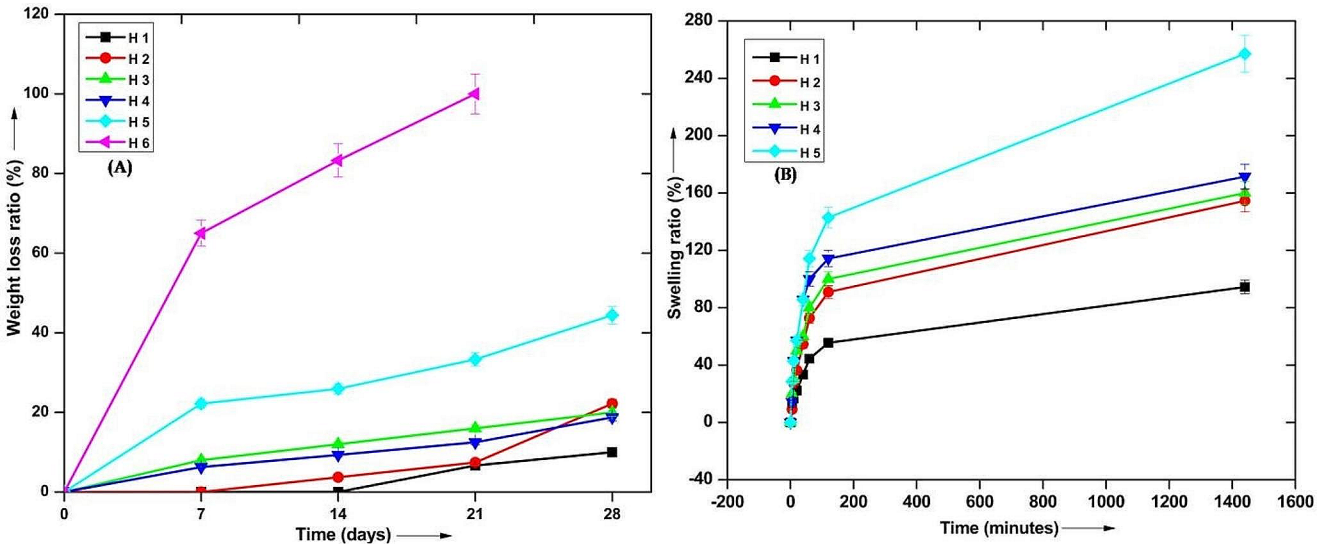

Fig. 3 Biodegradation studies of the hydrogels H1 to H6 (A), and Swelling studies of the hydrogels H1 to H5 (B); ($n = 3$)

Table 3 Tensile strength analysis of the hydrogels H1 to H5

Hydrogel Type	Ultimate Tensile Strength, UTS (MPa)	Percentage Extension
H1	2.25 ± 0.11	94 ± 4.7
H2	1.77 ± 0.08	64.4 ± 3.22
H3	1.70 ± 0.09	62.8 ± 3.46
H4	1.63 ± 0.08	66.8 ± 3.34
H5	1.35 ± 0.05	66.5 ± 3.32

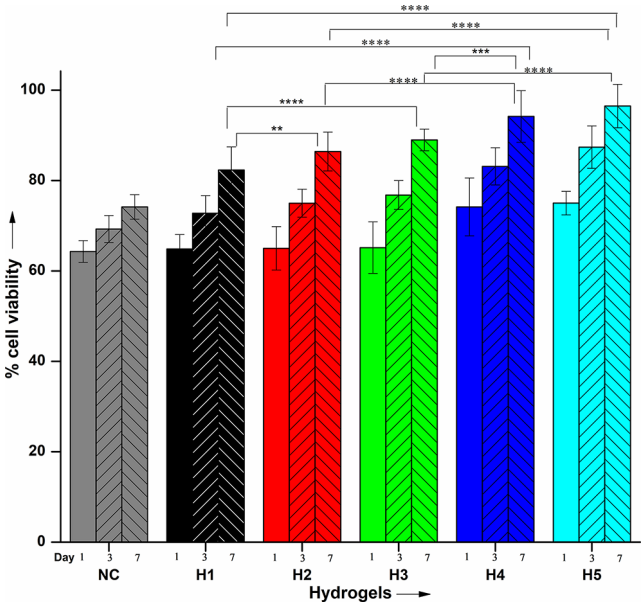

Fig. 4 Percentage cell viability seen on day 1, 3, and 7 in all the hydrogel groups (**$p \leq 0.05$, ***$p \leq 0.001$, ****$p \leq 0.0001$)

the hydrogels on increasing the Col-h content. A similar decrease was observed in hydrogels of fish collagen blend with PVA [37]. The lowering of the tensile strength values of the hydrogels from H1 to H5 can be due to their larger pore sizes (Table 2) which arise due to increase in Col-h content and leads to lower intermolecular interaction among the PVA chains, with subsequent decrease in tensile strength [38].

Antimicrobial activity evaluation

The raw ESM is known for its antibacterial properties due to the presence of lysozyme. In contrast, the ESM hydrolysates (prepared by chemical treatment) exhibit varying degrees of antibacterial activity [39]. Its assessment can enable an insight into the retention of this property within our hydrolysate fraction, prepared enzymatically. The hydrogel precursor solutions tested for their antibacterial activity against *E.coli* showed prominent inhibition zones of 15.08, 14.81, 16.93, and 17.46 mm for H3, H4, H5, and H6 respectively (depicted in ***Figure S2***). The abundance of proline in the Col-h, which is well known for its activity against gram negative bacteria, can also be another contributing factor [40]. In contrast, the solutions having lower Col-h content did not show any antibacterial activity, suggesting the role of hydrolysate concentration in achieving the desired antimicrobial effect.

In–vitro cell proliferation, cytotoxicity, and viability assessment

The biocompatibility of all the hydrogels was evaluated using seeded MG-63 osteoblasts. The cell viability results from the MTT assay (Fig. 4) concluded that the cell viability increased on increasing the Col-h content of the hydrogel sample groups; with H5 showing the maximum percentage of viable cells as 75.02% after day 1. The cells proliferated well during the one-week study, with viability reaching to a maximum of 96.5% in case of H5. The results were further compared through the statistical evaluation measures which confirmed significant differences in percentage cell viability between all sample types barring H2-H3, and H4-H5 (p-values for these pairs were greater than 0.05).

Henceforth, the cells grown in H3, H4, and H5 extracts were morphologically analyzed. The fluorescence images (Fig. 5) revealed that the cells had a normal elongated polygonal [41] morphology. The average cell size as computed using ImageJ [20], was 122.88 ± 20.74 µm, 136.43 ± 32.46 µm, and 100.18 ± 24.50 µm for H3, H4, and H5 respectively. The cell size increased from H3 to H4, as can also be observed through better cell spreading and cytoplasmic extensions in the latter case. The cells exhibited spindle and chained morphology. The size decreased in case of H5, (presence of more round and oval cells can be seen) which can be attributed to more amount of Col-h in this case. Higher Col-h might lead to increased binding with the integrin receptors of the cell surface, over a much shorter distance when compared with lower Col-h (receptor saturation model) [42]. High viability of cells was seen at day 7, which was in coherence with the results of the MTT assay, as discussed above.

Discussion

The Col-h based hydrogels were physically stable, along with their chemical composition which was revealed by ATR-FTIR measurements. The characteristic IR peaks supported the existence of both collagen and PVA moieties. The results were similar to hydrogels developed from fish collagen [28], ESM collagen dispersions [9], and type II collagen [26] along with PVA. The diffraction peaks, centered around $2\theta = 20°$ were also reported for collagen/PVA hydrogels, wherein the collagen was sourced from fish [28]. Their XRD data also revealed the

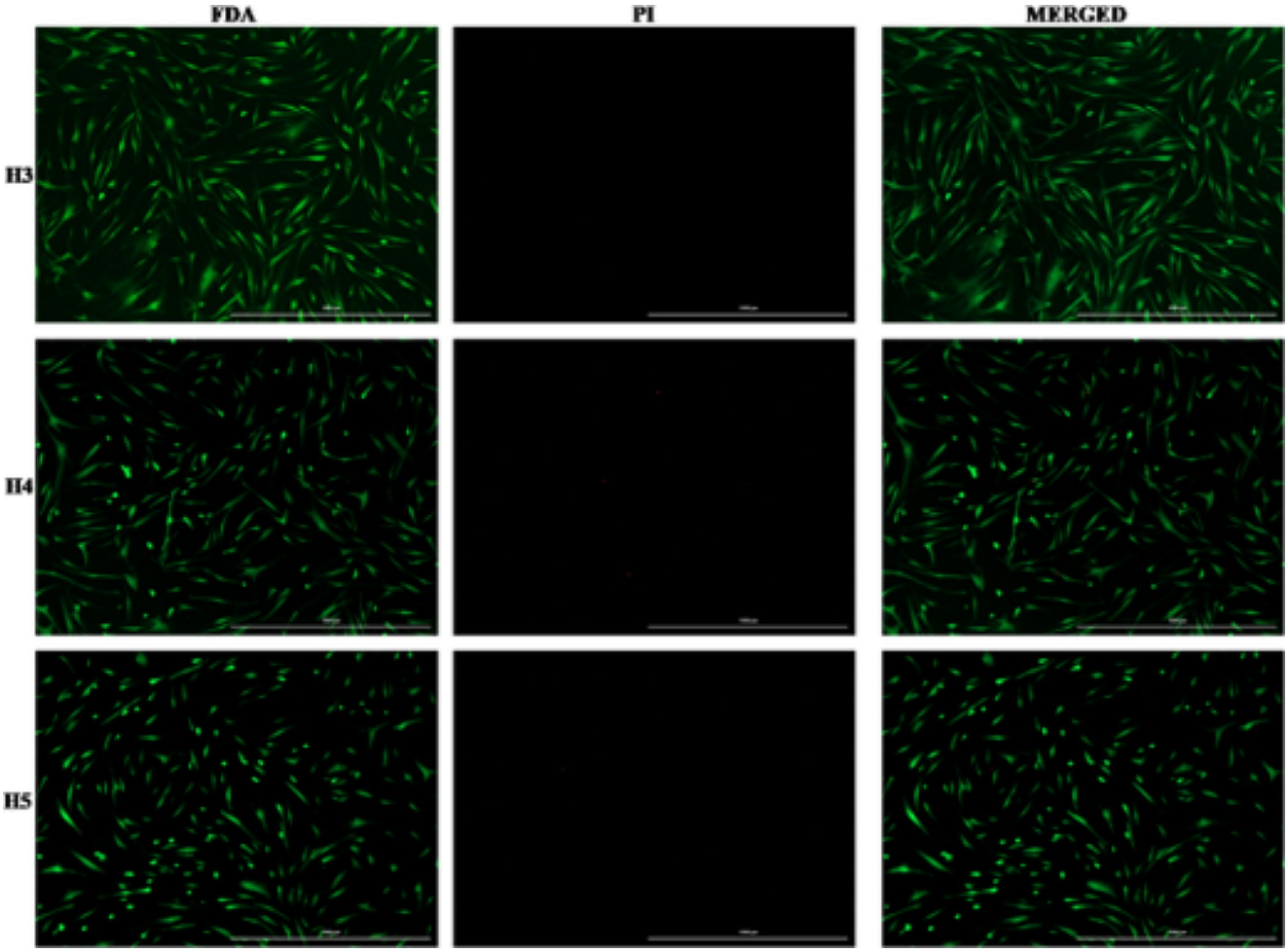

Fig. 5 Fluorescence microscopy images of MG-63 osteoblasts, cultured over H3, H4, and H5 hydrogel extracts for 7 days (scale bar = 1000 μm)

presence of PVA crystalline peaks which were retained in the hydrogels due to non-disruption of the molecular chains' geometric structure [28]. Furthermore, the results of the topological measurements were consistent with those obtained from collagen type II/PVA hydrogels [26]. These hydrogels also showed micro-dimensional pore sizes, which increased with increasing collagen content. The group also reported a similar increasing trend for percentage porosities, and average surface roughness [9] as also witnessed in our measurements.

The high swelling capacity of our hydrogels matched those of collagen/PVA composite patches [29]; which ranged between 237 and 503% after 24 h of immersion in PBS. The study also reported increased fluid uptake with increasing collagen content. The degradation rate of our hydrogels increased with the Col-h content, as also reported for collagen type II/PVA hydrogels utilized in cartilage TE [26]. The group reported a degradation rate of ~ 50% for 50:50 hydrogels, being very close to our rate of 44% for the same ratio of hydrogels after 28 days of study. In addition, the tensile strength values of our hydrogels were similar to the reported collagen/PVA composite patches utilized for osteochondral defects [29]. Preventing infections at the wounded site is imperative for the repair mechanism to continue effectively. The observed antimicrobial activity of our hydrogels might be due to the presence of antimicrobial peptides like avian β-defensins, histones, and Ovocalyxin-36 present in the avian ESM [43]. Bovine tendon extracted Type I collagen hydrolysate tested against *S. aureus and E. coli* also showed similar antimicrobial activity [40]. The comparatively greater percentage of viable cells in H5 could be attributed to the presence of a much more suitable physicochemical environment, with a greater amount of amino acids and arginine-glycine-aspartic acid (RGD) sequences known to be present in the ESM [44], and inherently responsible for cell adhesion and growth. The cellular morphology and percentage cell viability for H4 were insignificant in comparison to H5, whilst having a greater tensile strength, implying it to be the best among our samples to satisfy the characteristics of an efficient bone TE matrix.

Conclusion and future perspectives

The study presented the extraction and formation of collagen hydrolysate from chicken eggshell membrane, followed by hydrogel formation through crosslinking with PVA. The hydrogels' physic-chemical investigation revealed porous structures and interconnectivity, as well as the presence of cell-specific functional groups, which suggested their assistance in cell growth by allowing for accessible nutrition and gaseous exchange. The micro-dimensional features of the hydrogels like pore size and average surface roughness, in addition to optimum swelling and degradation rate can be conducive towards effective bone regeneration. Numerous research studies have demonstrated that the scaffold's micro-dimensional features facilitate and regulate multiple cellular processes, including improved osteo- and angiogenesis. Furthermore, the ultimate tensile strength of the hydrogels (1.3–2.2 MPa) suggested towards their applications in cartilaginous and osteochondral defects. In addition, the inherent antimicrobial properties of the Col-h can contribute towards combating infection at the repair site. Cell viability differences between H4 and H5 were not significant, and the UTS of H4 was higher; suggesting the use of Col-h/PVA in the ratio of 40:60 in particular, for developing different hydrogel systems for efficient bone restoration applications. The osteoblasts proliferated well, with only a few dead cells seen during live/dead assessment. Although these results were encouraging, it should be noted that these preliminary results clear the way to further investigate a three-dimensional encapsulation culture with developed hydrogel for effective bone tissue regeneration.

Supplementary Information The online version contains supplementary material available at https://doi.org/10.1007/s11033-024-09394-9.

Acknowledgements The authors are thankful to Prof. A. Chatterjee and Dr. Monica Sikka (Dept. of Textile Technology, NIT Jalandhar, India) for ATR-FTIR and tensile strength measurements respectively. Further, the authors acknowledge the support from Ministry of Human Resource and Development (Govt. of India) to Ms. Aakriti Aggarwal for scholarship.

Author contributions AA and MKS contributed to the study conception and design. Material preparation, data collection and analysis of developed materials were performed by AA and MKS while the biocompatibility study was performed by DN and AP with Serb funding. The first draft of the manuscript was written by AA and all authors commented on previous versions of the manuscript. All authors read and approved the final manuscript.

Funding Science and Engineering Research Board, Department of Science and Technology (Govt. of India) to the author Dr. Asish Pal and Mr. Debasish Nath for funding the cyto-toxicity studies.

Data availability The associated data can be made available by authors on request.

Declarations

Ethical approval No human/animal studies involved. The in-vitro cytotoxicity studies were performed with approval of Institutional Ethical Committed (IEC), Institute of Nanoscience and Technology, Mohali, India.

Competing interests The authors declare no competing interests.

References

1. Shang F, Yu Y, Liu S et al (2021) Advancing application of mesenchymal stem cell-based bone tissue regeneration. Bioact Mater 6:666–683. https://doi.org/10.1016/j.bioactmat.2020.08.014
2. Sah MK, Banerjee I, Pramanik K (2017) Eggshell Membrane Protein Modified Silk Fibroin-Poly Vinyl Alcohol Scaffold for bone tissue Engineering: in Vitro and in vivo study. J Biomim Biomater Biomed Eng 32:69–81. https://doi.org/10.4028/www.scientific.net/JBBBE.32.69
3. Lin X, Patil S, Gao Y-G, Qian A (2020) The bone extracellular matrix in bone formation and regeneration. Front Pharmacol 11
4. Hou Y, Jin M, Sun D et al (2023) Multifunctional inorganic/organic nanocomposite microspheres - reinventing eggs for bone repair applications. Compos Part B Eng 255:110644. https://doi.org/10.1016/j.compositesb.2023.110644
5. Wong SK, Yee MMF, Chin K-Y, Ima-Nirwana S (2023) A review of the application of Natural and Synthetic scaffolds in Bone Regeneration. J Funct Biomater 14:286. https://doi.org/10.3390/jfb14050286
6. Aggarwal A, Sah MK (2021) Chapter Three - Electrospun materials as scaffolds in tissue engineering and regenerative medicine. In: Kasoju N, Ye H (eds) Biomedical Applications of Electrospinning and Electrospraying. Woodhead Publishing, pp 83–121
7. Yousefiasl S, Sharifi E, Salahinejad E et al (2023) Bioactive 3D-printed chitosan-based scaffolds for personalized craniofacial bone tissue engineering. Eng Regen 4:1–11. https://doi.org/10.1016/j.engreg.2022.09.005
8. Moghanian A, Raz M, Miri Z et al (2023) Synthesis and characterization of mg and Sr-modified calcium phosphate/gelatin biomimetic scaffolds for bone tissue engineering. Ceram Int 49:18255–18263. https://doi.org/10.1016/j.ceramint.2023.02.197
9. Aggarwal A, Sah MK (2023) Fabrication of avian eggshell membrane derived dispersed collagen hydrogels for potential bone regeneration. J Polym Eng. https://doi.org/10.1515/polyeng-2023-0071
10. Aggarwal A, Sah MK (2022) Chap. 16 - eggshell membrane in skin tissue engineering and wound healing. In: Sah MK, Kasoju N, Mano JF (eds) Natural polymers in Wound Healing and Repair. Elsevier, pp 417–435
11. Zhu L, Xie Y, Wen B et al (2020) Porcine bone collagen peptides promote osteoblast proliferation and differentiation by activating the PI3K/Akt signaling pathway. J Funct Foods 64:103697. https://doi.org/10.1016/j.jff.2019.103697
12. Matinong AME, Chisti Y, Pickering KL, Haverkamp RG (2022) Collagen extraction from animal skin. Biology 11:905. https://doi.org/10.3390/biology11060905
13. Jiang H, Kong Y, Song L et al (2023) A thermostable type I collagen from swim bladder of silver carp (Hypophthalmichthys molitrix). Mar Drugs 21:280. https://doi.org/10.3390/md21050280
14. Park S, Kim T, Gwon Y et al (2019) Graphene-Layered Eggshell Membrane as a flexible and functional Scaffold for enhanced proliferation and differentiation of stem cells. ACS Appl Bio Mater 2:4242–4248. https://doi.org/10.1021/acsabm.9b00525

15. Chen X, Zhu L, Wen W et al (2019) Biomimetic mineralisation of eggshell membrane featuring natural nanofiber network structure for improving its osteogenic activity. Colloids Surf B Biointerfaces 179:299–308. https://doi.org/10.1016/j.colsurfb.2019.04.009
16. Park S, Gwon Y, Kim W, Kim J (2021) Rebirth of the Eggshell Membrane as a Bioactive Nanoscaffold for tissue Engineering. ACS Biomater Sci Eng 7:2219–2224. https://doi.org/10.1021/acsbiomaterials.1c00552
17. Torres-Mansilla A, Hincke M, Voltes A et al (2023) Eggshell Membrane as a Biomaterial for Bone Regeneration. Polymers 15:1342. https://doi.org/10.3390/polym15061342
18. Aggarwal A, Sah MK (2022) Process optimization for extraction of avian eggshell membrane derived collagen for tissue engineering applications. J Polym Eng. https://doi.org/10.1515/polyeng-2021-0315
19. Chen Y, Li J, Lu J et al (2022) Synthesis and properties of poly(vinyl alcohol) hydrogels with high strength and toughness. Polym Test 108:107516. https://doi.org/10.1016/j.polymertesting.2022.107516
20. Schneider CA, Rasband WS, Eliceiri KW (2012) NIH Image to ImageJ: 25 years of image analysis. Nat Methods 9:671–675. https://doi.org/10.1038/nmeth.2089
21. Hy Rel (2022) Analyzing and calculating the porosity of scaffolds - Hyrel 3D
22. Sharifi F, Hasani M, Atyabi SM et al (2022) Mesenchymal stem cells encapsulation in chitosan and carboxymethyl chitosan hydrogels to enhance osteo-differentiation. Mol Biol Rep 49:12063–12075. https://doi.org/10.1007/s11033-022-08013-9
23. Singh S, Garg S, Saran AD (2023) CdSe nanodots to nanorods in PVA films: effect of shape transition and loading on the optomechanical and biodegradation properties. J Polym Eng 43:715–728. https://doi.org/10.1515/polyeng-2023-0031
24. Gupta N, Singh A, Dey N et al (2021) Pathway-driven peptide–bioglass nanocomposites as the dynamic and self-healable matrix. Chem Mater 33:589–599. https://doi.org/10.1021/acs.chemmater.0c03757
25. Adelnia H, Ensandoost R, Shebbrin Moonshi S et al (2022) Freeze/thawed polyvinyl alcohol hydrogels: Present, past and future. Eur Polym J 164:110974. https://doi.org/10.1016/j.eurpolymj.2021.110974
26. Lan W, Xu M, Zhang X et al (2020) Biomimetic polyvinyl alcohol/type II collagen hydrogels for cartilage tissue engineering. J Biomater Sci Polym Ed 31:1179–1198. https://doi.org/10.1080/09205063.2020.1747184
27. Meireles Gouvêa Boggione D, Boggione Santos IJ, Menezes de Souza S, Santos Mendonça RC (2021) Preparation of polyvinyl alcohol hydrogel containing bacteriophage and its evaluation for potential use in the healing of skin wounds. J Drug Deliv Sci Technol 63:102484. https://doi.org/10.1016/j.jddst.2021.102484
28. Wang M, Li J, Li W et al (2018) Preparation and characterization of novel poly (vinyl alcohol)/collagen double-network hydrogels. Int J Biol Macromol 118:41–48
29. Iqbal B, Muhammad N, Rahim A et al (2019) Development of collagen/PVA composites patches for osteochondral defects using a green processing of ionic liquid. Int J Polym Mater Polym Biomater 68:590–596. https://doi.org/10.1080/00914037.2018.1474358
30. Been S, Choi J, Cho H et al (2021) Preparation and characterization of a soluble eggshell membrane/agarose composite scaffold with possible applications in cartilage regeneration. J Tissue Eng Regen Med 15:375–387. https://doi.org/10.1002/term.3178
31. Ricciardi R, Auriemma F, De Rosa C, Lauprêtre F (2004) X-ray diffraction analysis of poly(vinyl alcohol) hydrogels, obtained by freezing and thawing techniques. Macromolecules 37:1921–1927. https://doi.org/10.1021/ma035663q
32. Edikresnha D, Suciati T, Suprijadi, Khairurrijal K (2021) Freeze-thawed hydrogel loaded by Piper Crocatum extract with in-vitro antibacterial and release tests. J Mater Res Technol 15:17–36. https://doi.org/10.1016/j.jmrt.2021.07.151
33. Ebrahimi M (2021) Porosity parameters in biomaterial science: definition, impact, and challenges in tissue engineering. Front Mater Sci 15:352–373. https://doi.org/10.1007/s11706-021-0558-4
34. Selvakumar G, Lonchin S (2020) Fabrication and characterization of collagen-oxidized pullulan scaffold for biomedical applications. Int J Biol Macromol 164:1592–1599. https://doi.org/10.1016/j.ijbiomac.2020.07.264
35. Marin Ștefania A, Kaya MG, Ghica MV et al (2018) Collagen-polyvinyl alcohol-Indomethacin Biohybrid matrices as Wound Dressings. Pharmaceutics 10:224. https://doi.org/10.3390/pharmaceutics10040224
36. Mahnama H, Dadbin S, Frounchi M, Rajabi S (2017) Preparation of biodegradable gelatin/PVA porous scaffolds for skin regeneration. Artif Cells Nanomed Biotechnol 45:928–935. https://doi.org/10.1080/21691401.2016.1193025
37. Punjataewakupt A, Reddy N, Aramwit P (2022) Enhancing clinical applications of PVA hydrogel by blending with collagen hydrolysate and silk sericin. J Polym Res 29:110. https://doi.org/10.1007/s10965-022-02965-z
38. Hartatiek, Fathurochman F, Wuriantika MI et al (2023) Mechanical, degradation rate, and antibacterial properties of a collagen-chitosan/PVA composite nanofiber. Mater Res Express 10:025401. https://doi.org/10.1088/2053-1591/acb990
39. Pillai MM, Saha R, Tayalia P (2023) Avian eggshell membrane as a material for tissue engineering: a review. J Mater Sci 58:6865–6886. https://doi.org/10.1007/s10853-023-08434-2
40. Ramadass SK, Perumal S, Gopinath A et al (2014) Sol–Gel assisted fabrication of collagen Hydrolysate Composite Scaffold: a Novel Therapeutic Alternative to the traditional collagen Scaffold. ACS Appl Mater Interfaces 6:15015–15025. https://doi.org/10.1021/am502948g
41. Chatree K, Sriboonaied P, Phetkong C et al (2023) Distinctions in bone matrix nanostructure, composition, and formation between osteoblast-like cells, MG-63, and human mesenchymal stem cells, UE7T-13. Heliyon 9:e15556. https://doi.org/10.1016/j.heliyon.2023.e15556
42. Wu I-C, Liou J-W, Yang C-H et al (2023) Self-assembly of gelatin and collagen in the polyvinyl alcohol substrate and its influence on cell adhesion, proliferation, shape, spreading and differentiation. Front Bioeng Biotechnol 11:1193849. https://doi.org/10.3389/fbioe.2023.1193849
43. Ahmed TAE, Suso H-P, Hincke MT (2017) In-depth comparative analysis of the chicken eggshell membrane proteome. J Proteom 155:49–62. https://doi.org/10.1016/j.jprot.2017.01.002
44. Sah MK, Rath SN (2016) Soluble eggshell membrane: a natural protein to improve the properties of biomaterials used for tissue engineering applications. Mater Sci Eng C Mater Biol Appl 67:807–821. https://doi.org/10.1016/j.msec.2016.05.005